

## Detection of Double White Dwarf Binaries with *Gaia*, LSST and *eLISA*

Valeriya Korol,<sup>1</sup> Elena M. Rossi,<sup>1</sup> and Paul J. Groot<sup>2</sup>

<sup>1</sup>*Leiden Observatory, Leiden University, PO Box 9513, 2300 RA, Leiden, the Netherlands; korol@strw.leidenuniv.nl, emr@strw.leidenuniv.nl*

<sup>2</sup>*Department of Astrophysics, IMAPP, Radboud University, PO Box 9010, 6500 GL, Nijmegen, the Netherlands; p.groot@astro.ru.nl*

**Abstract.** According to simulations around  $10^8$  double degenerate white dwarf binaries are expected to be present in the Milky Way. Due to their intrinsic faintness, the detection of these systems is a challenge, and the total number of detected sources so far amounts only to a few tens. This will change in the next two decades with the advent of *Gaia*, the LSST and *eLISA*. We present an estimation of how many compact DWDs with orbital periods less than a few hours we will be able to detect 1) through electromagnetic radiation with *Gaia* and LSST and 2) through gravitational wave radiation with *eLISA*. We find that the sample of simultaneous electromagnetic and gravitational waves detections is expected to be substantial, and will provide us a powerful tool for probing the white dwarf astrophysics and the structure of the Milky Way, letting us into the era of multi-messenger astronomy for these sources.

### 1. Introduction

White dwarfs (WD) represent the most common final stellar fate. According to simulations the Milky Way should contain around  $10^{10}$  WDs (Napiwotzki 2009), among which  $10^8$  are in double white dwarf binaries (DWDs) (Nelemans et al. 2001). About half of these systems have periods shorter than 10 hours, so that gravitational waves (GW) emission will bring them into contact within a Hubble time, making them the most numerous low-frequency (0.1 mHz - 1 Hz) GW sources in the Galaxy and candidate progenitors for type Ia supernovae (SN Ia) (Iben & Tutukov 1984; Nelemans et al. 2001; Nissanke et al. 2012).

In the conventional picture of binary evolution, a binary needs to experience at least two phases of mass transfer to form a DWD. To form a short-period DWD binary, at least one mass-transfer phase needs to be a common envelope (Paczynski 1976; Webbink 1984). The subsequent evolution of the compact binary is driven by emission of orbital angular momentum through GW radiation, that slowly brings the two binary components together. The only two physical processes, expected to influence the binary evolution at very late stages and determine the final fate of the system are tidal interaction and mass transfer. The effects of tides become important at orbital periods of a few tens of minutes, and the onset of the mass transfer occurs at a period of about 10 min. The final fate of the binary depends on the stability of these two processes:

in almost all cases the binary system will merge, in the remaining fraction of cases the binary will survive as an AM CVn system (e.g., Solheim 2010).

Such an evolutionary path makes these systems key objects for testing binary evolution theories, and, in particular, predictions for the common envelope and the merger outcome. Moreover, they are guaranteed sources for the *eLISA* (evolved Laser Interferometer Space Antenna) mission (Amaro-Seoane et al. 2012). Finally, detached DWDs with orbital periods in the range from one hour to a few minutes are particularly suited for study the physics of tides, the stability of the mass-transfer process in compact binaries, and the role of these processes on the final fate of these systems. The detection of new systems will allow us to investigate these open questions.

Due to their intrinsic faintness, DWDs are very hard to find, and the total number of detected sources so far amounts only to a few tens. Future progress in the detection of these sources with *Gaia* (*Gaia* Collaboration 2016), the LSST (Large Synoptic Survey Telescope) (LSST Science Collaboration et al. 2009) and the *eLISA* mission was highlighted by several authors, but has never been quantified. Here we present an estimate of a sample of Galactic ultracompact detached DWD binaries that could be obtained with these instruments.

## 2. Electromagnetic Detections

For the EM detections we focus our analysis on two instruments: *Gaia* and LSST. Being extensive photometric surveys, both are expected to strongly contribute to the detection of new eclipsing DWDs (Eyer et al. 2012).

As a first step in our simulation we model the Galactic population of DWDs by using the binary population synthesis code SeBa, developed by Portegies Zwart & Verbunt (1996), for more updated versions see Nelemans et al. (2001) and Toonen et al. (2012). To take into account the star formation history of the Galaxy we used a code originally developed by Nelemans et al. (2004), in which star formation rate is modeled as a function of time and position based on Boissier & Prantzos (1999, see Equations 1-2 of Nelemans et al. 2004). The absolute magnitudes for WDs are deduced from the WD cooling models of Hansen (1999), and corrected for extinction according to Schlegel et al. (1998).

As a next step we model the light curves of the obtained DWD population by using a simple geometrical model, in which we compute the flux of the binary for given binary parameters. In this simple treatment the limb darkening effect, gravitational distortion (ellipsoidal variation) and mutual heating are not taken into account. The initial orbital phase and the inclination angle of the orbit with respect to plane of the sky are assigned randomly. We applied a colour-colour polynomial transformation in order to convert Sloan *r*-band magnitudes into *Gaia* *G* magnitude with coefficients according to Carrasco et al. (2014, Table 6). To evaluate the relative photometric error we use<sup>1</sup>:

$$\sigma_G = 10^{-3}(0.04895z^2 + 1.8633z + 0.00001985)^{1/2}, \quad (1)$$

where  $z = \max[10^{0.4(12-15)}, 10^{0.4(G-15)}]$ . To evaluate an expected photometric error per single observation with the LSST we use

$$\sigma_r = (\sigma_{\text{sys}}^2 + \sigma_{\text{rand}}^2)^{1/2}, \quad (2)$$

---

<sup>1</sup><http://www.cosmos.esa.int/web/gaia/science-performance>

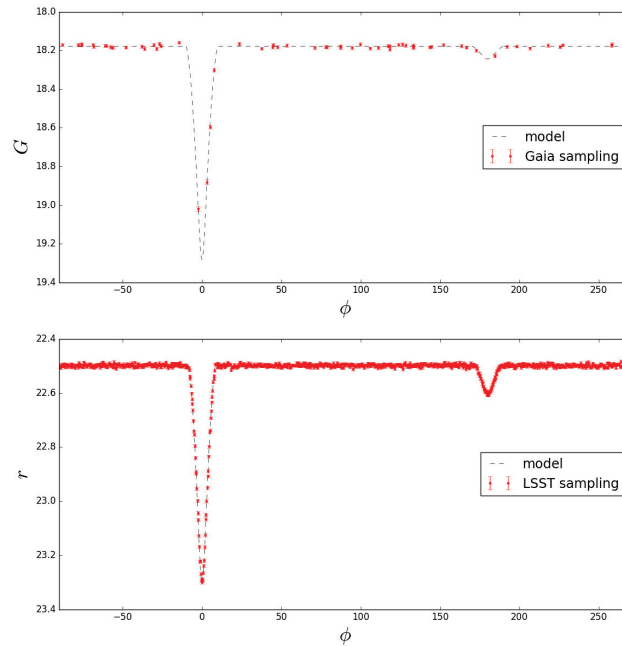


Figure 1. An example of phase folded light curves sampled with *Gaia* observations (top panel) and LSST observations (bottom panel). Periods of the two sources are respectively  $P \simeq 21$  min and  $P \simeq 24$  min.

where, according to LSST Science Collaboration et al. (2009, Section 3.5),  $\sigma_{\text{sys}} = 0.005$ ,  $\sigma_{\text{rand}}^2 = (0.04 - \gamma)x + \gamma x^2$ ,  $x = 10^{(m-m_5)}$ ,  $m_5$  and  $\gamma$  are respectively the  $5\sigma$  limiting magnitude for a given filter and the sky brightness in a given band. Finally, we apply Gaussian white noise to our sample of light curves.

To get a realistic light curve sampling for *Gaia*, we used The *Gaia Observation Forecast Tool*<sup>2</sup>, that provides a list of observing times per target for a given period of observation and target position in the sky. To simulate the light curve sampling with the LSST we use the nominal cadence of 3 days over a nominal ten-year life span of the mission. Fig. 1 shows a comparison of the light curve sampling with *Gaia* (top panel) and LSST (bottom panel) for two binaries with a similar orbital period. As a detection test we check if a source presents variability by evaluating the  $\chi^2$  value of the light curve with respect to the average source magnitude. We required a minimum number of data points with  $5\sigma$  significance to sample the eclipse: at least 3 observations for *Gaia* and 10 observations for the LSST.

In our simulation we find 220 eclipsing sources detected with *Gaia*, and 6230 detected with LSST. Both instruments will detect a population of DWD with orbital periods less than one day, with  $\sim 90\%$  of detections having an orbital period less than a few hours, up to the maximum distance of 2.5 kpc with *Gaia* and 12 kpc with LSST. In Fig. 2 we show the characteristics of detected DWD population and its distribution in the Galaxy: the magnitude-period distribution (top panels), distribution with Galac-

<sup>2</sup><http://gaia.esac.esa.int/gost/>

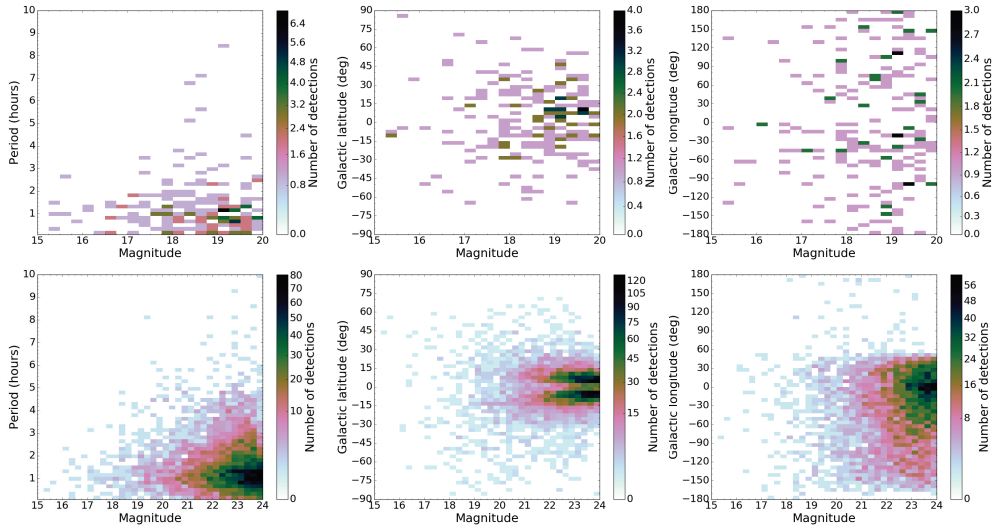


Figure 2. Contour plot for the number of detections in different 2D parameter spaces: upper panels for *Gaia*, lower panels for LSST. The color indicates the number of detected sources.

tic latitude (middle panels) and longitude (bottom panels), where colour indicates the number of detected sources.

### 3. Gravitational Wave Detections

As pointed out by several authors, DWDs are expected to be the most numerous GW source in the Galaxy detectable with an *eLISA*-like interferometer. In principle, considering that the timescale on which these systems typically evolve is much larger ( $> \text{Myr}$ ) than the lifetime of the mission ( $\sim \text{yr}$ ), they can be treated as monochromatic sources. The gravitational waves they produce can be computed using the quadrupole approximation (e.g., Peters & Mathews 1963).

For each binary in our simulation we compute the signal-to-noise ratio as the averaged orbit GW amplitude, adopting the method from Cornish & Larson (2003)<sup>3</sup>, over the average noise level at the binary frequency. To estimate the noise level at the source frequency we use the analytic fit to the sky-averaged sensitivity curves of an *eLISA*-like detector from Klein et al. (2016), that allow to model different detector designs: from the minimal *eLISA* configuration (Amaro-Seoane et al. 2012) to the original *LISA* mission (Prince et al. 2006). Note, that the main difference between *eLISA* and *LISA* configurations is a different number of arms and different arm lengths. Both missions are conceived as a set of three spacecrafts in an equilateral triangle. In the *LISA* configuration the separation between spacecrafts is 5 Mkm and all three spacecrafts are connected by laser links, while in the *eLISA* mission spacecrafts are separated by 1 Mkm and only two sides of the triangle are connected by laser links. To model the

<sup>3</sup>This method takes into account sky position, orientation of the source to the detector and annual modulation of the signal due to the orbital motion of the detector.

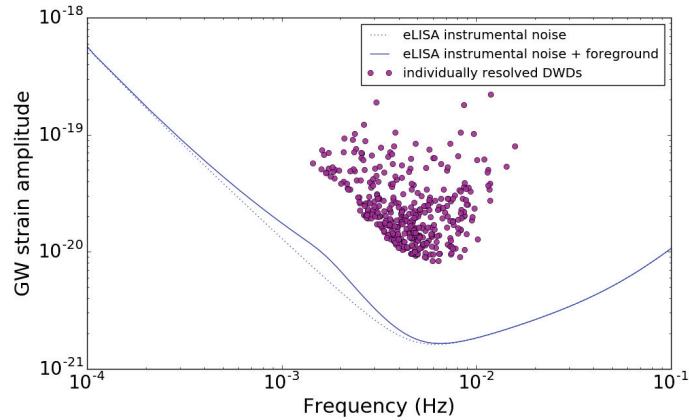


Figure 3. GW signal from a sample of Galactic DWDs with  $\text{SNR} > 5$ , the solid line represent *eLISA* sensitivity curve, that includes the instrumental noise and the foreground signal from unresolved DWD binaries.

foreground noise component, produced by unresolved DWD binaries, we use an analytical prescription from Nissanke et al. (2012) and we add it to the instrumental noise in quadrature. Fig. 3 illustrates the obtained sensitivity curve for the *eLISA* configuration and the sample of detected binaries detected with SNR threshold of 5. We estimate the number of individually resolved DWDs binaries with  $\text{SNR} > 5$  to be  $2.5 \times 10^3$  for the *eLISA* 2 yr mission and  $20 \times 10^3$  for the classic *LISA* 5 yr mission. Orbital periods of the detected binaries range from 5 min to 1.5 h.

#### 4. Simultaneous Electromagnetic and Gravitational Wave Detections

Finally, we estimate the combined EM and GW sample, i.e. the sample of DWDs detected with *Gaia* and *LSST* that are bright enough in GWs to be detected with an *eLISA*-like experiment. We repeat the same procedure described in Sect. 3 to compute the SNR in GWs for *Gaia* and *LSST* detected eclipsing binaries. We find that *Gaia* will provide several tens of EM counterparts and *LSST* will provide several thousands EM counterparts for the *eLISA* mission. The exact number of detections depends on the configuration of the GW interferometer. Fig. 4 shows EM properties of this sample.

#### 5. Conclusions

Large sample of simultaneous EM and GW detections will significantly extend the sample of *eLISA* verification binaries, i.e. well known ultracompact binaries that are expected to be detected in a very short time after the beginning of the mission and can be used to verify the performance of the instrument. This sample will provide us an opportunity of multi-messenger study for this class of objects, since no other GW sources are expected to provide so large number of simultaneous GW and EM detections. Ultimately, we will have a powerful tool for probing the physics of WDs and we will be able to map the Galactic potential by combining EM and GW data.

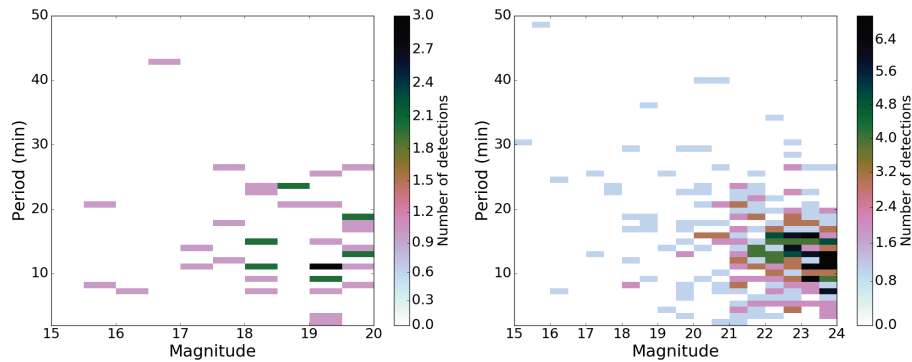


Figure 4. Contour plot for simultaneous GW and EM detections as a function of binary parameters.

**Acknowledgments.** We are grateful to Gijs Nelemans, Silvia Toonen, Anthony Brown and Alberto Sesana for useful discussions. This work was supported by NWO WRAP Program.

## References

- Amaro-Seoane, P., Aoudia, S., Babak, S., et al. 2012, *Classical and Quantum Gravity*, 29, 124016
- Boissier, S., & Pranzos, N. 1999, *MNRAS*, 307, 857
- Carrasco, J. M., Catalán, S., Jordi, C., et al. 2014, *A&A*, 565, A11
- Cornish, N. J., & Larson, S. L. 2003, *Phys.Rev.D*, 67, 103001
- Eyer, L., Dubath, P., Mowlavi, N., et al. 2012, *From Interacting Binaries to Exoplanets: Essential Modeling Tools*, 282, 33
- Gaia Collaboration, Prusti, T., de Bruijne, J. H. J., et al. 2016, *A&A*, 595, A1
- Hansen, B. M. S. 1999, *ApJ*, 520, 680
- Marsh, T. R., Nelemans, G., & Steeghs, D. 2004, *MNRAS*, 350, 113
- Napiwotzki, R. 2009, *Journal of Physics Conference Series*, 172, 012004
- Nelemans, G., Yungelson, L. R., Portegies Zwart, S. F., & Verbunt, F. 2001, *A&A*, 365, 491
- Nelemans, G., Yungelson, L. R., & Portegies Zwart, S. F. 2004, *MNRAS*, 349, 181
- Nissanke, S., Vallisneri, M., Nelemans, G., & Prince, T. A. 2012, *ApJ*, 758, 131
- Iben, I., Jr., & Tutukov, A. V. 1984, *ApJS*, 54, 335
- Klein, A., Barausse, E., Sesana, A., et al. 2016, *Phys.Rev.D*, 93, 024003
- LSST Science Collaboration, Abell, P. A., Allison, J., et al. 2009, *arXiv:0912.0201*
- Paczynski, B. 1976, *Structure and Evolution of Close Binary Systems*, 73, 75
- Peters, P. & Mathews, J. 1963, *Phys. Rev.*, 131, 435
- Portegies Zwart, S. F., & Verbunt, F. 1996, *A&A*, 309, 179
- Prince, T. A., Binetruy, P., Centrella, J., et al. 2006, *Bulletin of the American Astronomical Society*, 38, 74.01
- Schlegel, D. J., Finkbeiner, D. P., & Davis, M. 1998, *ApJ*, 500, 525
- Solheim, J.-E. 2010, *PASP*, 122, 1133
- Toonen, S., Nelemans, G., & Portegies Zwart, S. 2012, *A&A*, 546, A70
- Webbink, R. F. 1984, *ApJ*, 277, 355